Journal of Nuclear Materials 386–388 (2009) 564–568

Contents lists available at ScienceDirect

Journal of Nuclear Materials

journal homepage: www.elsevier.com/locate/jnucmat

Effect of thermal ageing on the impact fracture behaviour of Eurofer'97 steel

Hynek Hadraba *, Ivo Dlouhy

Institute of Physics of Materials, Academy of Sciences of the Czech Republic, Zizkova 22, 616 62 Brno, Czech Republic

ARTICLE INFO

PACS:
62.20.Mk

ABSTRACT

Ferritic–martensitic reduced activation steel Eurofer'97 is candidate structural material for in-vessel components of proposed fusion reactors. The use of the steel is limited up to a temperature about 550 °C. On the other hand the efficiency enhancement of the fusion reactors to the level suitable for energy production is predetermined by an increase of temperature in reactor. The long-term exposition of the steel at high temperatures leads to microstructural changes. The aim of the work was to investigate the influence of thermal ageing on fracture properties of Eurofer'97 steel. Thermal ageing of the steel was simulated by step cooling treatment. Charpy impact tests were performed before and after thermal ageing. No evident changes in impact properties have been registered when comparing the properties of the steel in as-received state and in state after step cooling.

1. Introduction

Ferritic–martensitic steels of (9–12)Cr–1Mo(W–Ni–V) type were developed for high temperature applications in nuclear power industry. These steels are nowadays under consideration as structural materials for perspective power sources: (i) fission reactors based on ^{235}U a ^{232}Th cycles [1], (ii) acceleration driven systems [2] and (iii) fusion reactors with magnetic plasma confining [3]. Several versions of RAFM (reduced activation ferritic–martensitic) steel of (9–12)Cr-X type have been developed in Europe [4,5], Japan [6,7], USA [1] and China [8]. The most advanced version, the 9Cr–1 W(V–Ta) Eurofer'97 steel, was selected as a structural material for DEMO fusion power plant prototype in-vessel and first wall components (outboard blanket) [4].

Operational embrittlement and subsequent brittle behaviour of the steels used in nuclear power industry is affected by synergy of two main influences: thermal and radiation damage. Radiation damage of the Eurofer'97 steel and elimination of its effect on mechanical properties is broadly studied as a preferred problem. There are also microstructural changes connected with operation temperatures (considered in the range 550–650 °C) such as carbidic reactions, grain coarsening and grain boundary embrittlement [9,10]. Detailed understanding of failure mechanism of Eurofer'97 steel in as-received thermally unaffected state and state after thermal ageing is critical for its proposed future applications.

The subgrain structure of Eurofer'97 steel in the as-received state composed of martensite laths of thickness ca. 200 nm. Also two main populations of carbides were identified in microstructure: Cr-rich carbides of the type $M_{23}C_6$, predominantly located on boundaries of prior austenite grains and martensite laths, and Ta and V-rich carbides of MX type located particularly inside of martensite laths [11]. Outstanding microstructural changes of Eurofer'97 steel after thermal ageing have been described, even at the temperatures lower than considered for application [10,12]. Coarsening of martensite laths, coarsening of carbides and segregation of P to grain boundaries was observed in particular already after 1000 h thermal ageing at 500 °C and 600 °C. It seems that segregation of P on grain boundary was connected with coarsening of carbides. Carbide coarsening caused Cr depletion of grain boundaries and allowed subsequent P segregation. The steel was also after 10000 h of thermal ageing partially recrystallized to equiaxed ferrite grains of diameter ca. 1 μm decorated by coarse (up to 350 nm) $M_{23}C_6$ carbides.

The temperature dependence of impact energy for 14 mm sheet of Eurofer'97 in the as-received state including scatter band of data collected from literature [10,13–15] is given in Fig. 1. Data representing the influence of long-term thermal ageing on impact energy of 14 mm Eurofer'97 steel published in literature [10,12] are also compiled in Fig. 1. It is evident, that relatively short-term thermal ageing 5000 h at 500 °C and 600 °C led to t_{DBTT} shift ca. +10 °C and +15 °C, respectively (t_{DBTT} was −65 °C for 14 mm sheet in as-received state). The long-term thermal ageing at 10000 h at 500 °C and 600 °C led to t_{DBTT} shift ca. +20 °C and +25 °C, respectively. The slight t_{DBTT} shift after short-term thermal ageing at 5000 h and the evident t_{DBTT} shift after long-term thermal ageing at 10000 h were explained just by partial recrystallization of martensite matrix to the ferrite grains [10,12]. The effect of P segregation observed already after short-term (1000 h) ageing was not described in literature, whereas this mechanism could lead to anomalous fracture behaviour. Grain boundary impurities

* Corresponding author. Tel.: +420 532 290 369; fax: +420 541 218 657.
E-mail address: hadraba@ipm.cz (H. Hadraba).

0022-3115/$ - see front matter © 2009 Elsevier B.V. All rights reserved.
doi:10.1016/j.jnucmat.2008.12.319

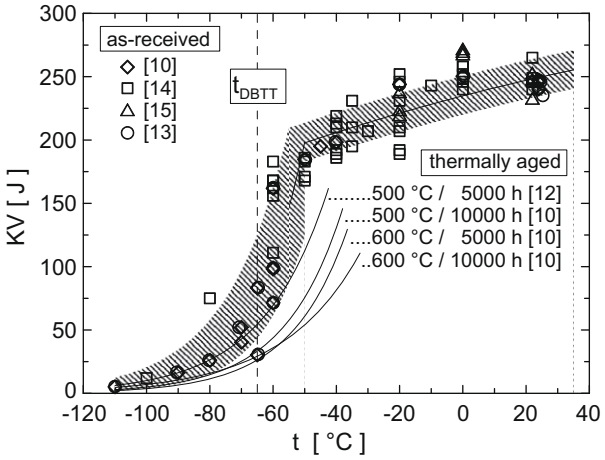

Fig. 1. Charpy impact energy temperature diagram of 14 mm sheet of Eurofer'97 in as-received state and after long-term thermal ageing.

enrichment leads generally to decrease of grain cohesion and consequently to intergranular fracture [16].

The aim of the work was to investigate the impact fracture behaviour and describe influence of short-term thermal ageing on fracture properties of Eurofer'97 steel.

2. Experimental procedure

2.1. Material

Two sheets of different thickness (14 and 25 mm) of Eurofer'97 steel were used for experiments. The sheets supplied by Böhler-Uddeholm originated from two different heats: heat nr. 993393 (sheet of tk. 14 mm) and heat nr. 993402 (sheet of tk. 25 mm). The chemical composition of the sheets was verified by emission spectral analysis (Spectrumat GDS 750, Leco).

The microstructure of Eurofer'97 sheets was observed in sections perpendicular to rolling direction by means of light optical (BX 51, Olympus) and scanning electron microscopy (JSM 6460, Jeol). The standard metallographic procedure was used for metallographic specimens preparations. Microstructure was then chemically etched and prior austenite grain size was evaluated according to ASTM standard E112.

Short-term thermal ageing (caused mainly by P segregation on grain boundary) was simulated by means of step cooling treatment. Procedure used in this work was developed and proven for P segregation in martensitic EM-10 steel of 9Cr–1Mo(Ni) type [2]. The applied step cooling treatment consisted of five stages: 650 °C/1 h, 590 °C/15 h, 575 °C/24 h, 550 °C/48 h and 520 °C/72 h.

2.2. Mechanical testing

Fracture behaviour of Eurofer'97 steel was studied on the steel in the as-received and in the step-cooled state by means of standard Charpy V-notch specimens tested in temperature range between −110 °C and +22 °C. The instrumented Charpy pendulum (Zwick/Roell) was used enabling to obtain load-deflection curves and determine additional fracture characteristics: yield force F_{gy}, maximum force F_m and t_{gy} temperature (defined as temperature of coincidence of general yield force F_{gy} and fracture force F_m on their temperature dependence).

Fracture surfaces were studied by means of light optical (BX 51, Olympus) and scanning electron microscopy (JSM 6460, Jeol) enabling to recognize fracture initiation site and to identify fracture propagation mechanism.

3. Results and discussion

3.1. Microstructure characterization

The chemical composition of 14 mm and 25 mm sheets used corresponded to nominal chemical composition of Eurofer'97 steel except the double content of molybdenum and alumina (see Table 1). The content of phosphorus was lower than the Eurofer'97 steel specification requires. The content of nickel exceeded three times the required level in the case of examined materials. The question is how these differences in the chemical composition can affect microstructural features and fracture behaviour of Eurofer'97 steel.

The thermal treatment of as-received sheets consisted of austenitization (980 °C/21.6 min/air) and subsequent annealing (760 °C/90 min/air). The microstructure of 14 mm and 25 mm Eurofer'97 sheets in the as-received state was then fully martensitic (see Fig. 2) with equiaxed prior austenitic grain size 8.3 ± 0.5 μm and 8.3 ± 1.0 μm, respectively. These values were comparable to the results published by Fernandez et al. [11]: 8.8 ± 2.2 μm for the 14 mm sheet and 8.7 ± 0.7 μm for 25 mm sheet. The prior austenite grains were decorated by carbides that corresponded mainly to Cr-rich $M_{23}C_6$ carbides of size up to 200 nm. This result was in accordance with results obtained by Fernandez et al. [11] which denotes $M_{23}C_6$ carbides sizes distribution frequency in Eurofer'97 from 25 nm to 210 nm with mean value of 75 nm.

Neither optical nor scanning electron microscopy enables any change in the microstructure of Eurofer'97 to be observed, between the as-received and the step-cooled state. The conditions of thermal ageing simulation were selected mainly with respect to effect of P segregation to grain boundaries and its effect to fracture behaviour of Eurofer'97 steel. Considering the analytical method applied for microstructure evaluation it was impossible to verify the presence of P on grain boundaries, especially in the case of low phosphorus content in the Eurofer'97 steel.

3.2. Fracture behaviour

The radiation damage and its effect on mechanical properties of Eurofer'97 steel was studied at literature broadly [17,18]. For evaluation of the radiation damage influence on fracture properties the Charpy V-notch test is widely used as a standard method. This was the main reason why the Charpy test is also used for evaluation of effect of thermal ageing on mechanical properties. Nevertheless the Charpy test application only without any of additional method of fracture behaviour characterization is questionable [13], among others because of in-plane and out-of-plane effects [19,20].

Table 1
Chemical composition of Eurofer'97 steel sheets used in wt%.

Element	C	Cr	W	V	Ta	Mn	Si	Ni	Mo	Al	P
Nominal	0.09	8.5	1.00	0.15	0.10	0.20	0.05	0.01	0.005	0.01	Maximum
Composition	0.12	9.5	1.20	0.25	0.14	0.60					0.005
14 mm sheet	0.11	8.7	1.07	0.23	0.12	0.55	0.03	0.03	0.01	0.02	0.001
25 mm sheet	0.11	8.8	1.09	0.23	0.14	0.56	0.03	0.03	0.01	0.02	0.003

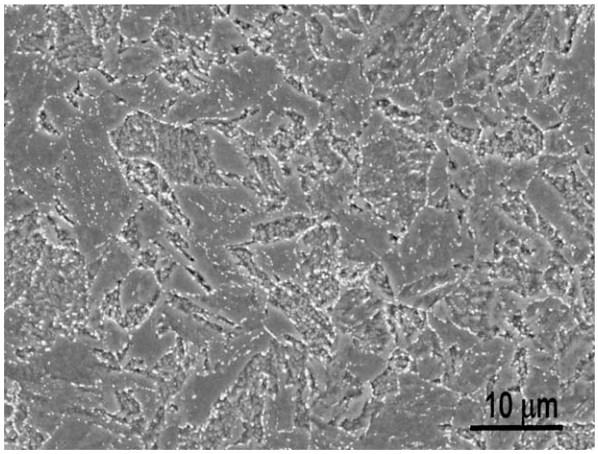

Fig. 2. Microstructure of 14 mm Eurofer'97 steel in as-received state.

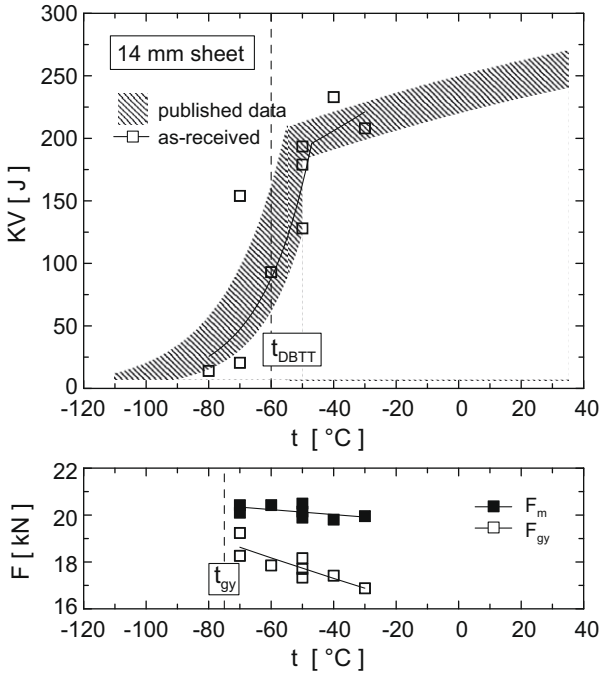

Fig. 3. Charpy impact energy temperature diagram of 14 mm sheet of Eurofer'97 in as-received state (upper – thermal dependance of impact energy, lower – temperature dependance of F_{gy} and F_m).

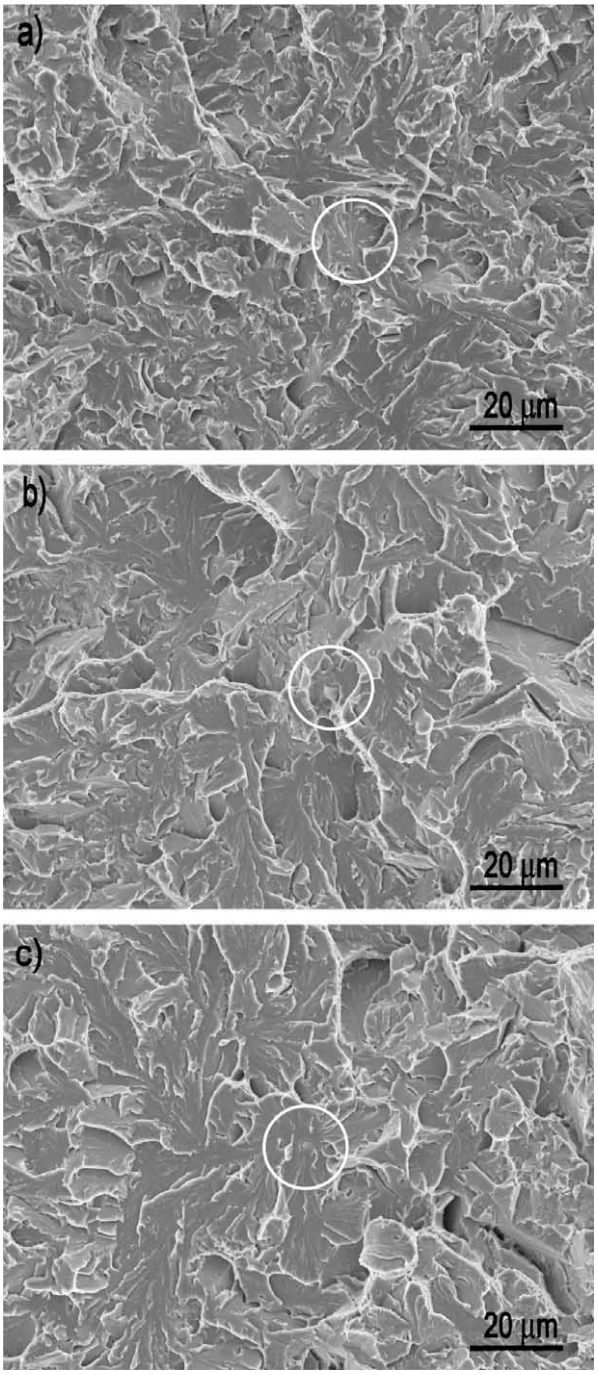

Fig. 4. Fracture surface of Eurofer'97 steel in the surrounding of initiation site (encircled) (a – 14 mm sheet in as-received state, b – 25 mm sheet in as-received state, c – 25 mm sheet in step-cooled state).

The measured temperature dependence of absorbed energy for 14 mm sheet compared with values collected from literature is given in Fig. 3. It is evident that the impact energy of 14 mm Eurofer'97 steel was comparable with published results. t_{DBTT} temperature was close to the literature data (see Fig. 1) and was about −60 °C. Data obtained from instrumented Charpy impact tester made possible to determine general yield temperature t_{gy} of 14 mm sheet. t_{gy} determined from the temperature dependence of general yield force F_{gy} and maximum force F_m given in the lower part of Fig. 3, was about −75 °C. The cleavage mechanism of crack initiation and propagation in Eurofer'97 steel in the as-received state under the conditions of brittle fracture (near t_{gy} temperature) was identified (see Fig. 4(a)) by means of microscopic examinations of fracture surfaces.

The measured thermal dependence of impact energy for 25 mm sheet in the as-received state compared with values for 14 mm sheet is given in Fig. 5. A completely different fracture behaviour of 25 mm sheet compared with 14 mm one was observed. The transition temperature t_{DBTT} of 25 mm sheet was shifted by ca. +20 °C to the temperature −45 °C and upper shelf energy level of 25 mm sheet was higher by about +50 J. In the as-received state the temperature curve obtained for 25 mm sheet embodied very sharp transition and larger scatter than transition temperature curve for 14 mm sheet. The F_{gy} and F_m forces of the 25 mm sheet reached lower values than in the case of 14 mm sheet. It is evident from thermal dependance of F_{gy} and F_m given in lower part of Fig. 5, that no change of t_{gy} temperature was observed in the case of 25 mm sheet comparing to 14 mm sheet. Microfractographic examin-

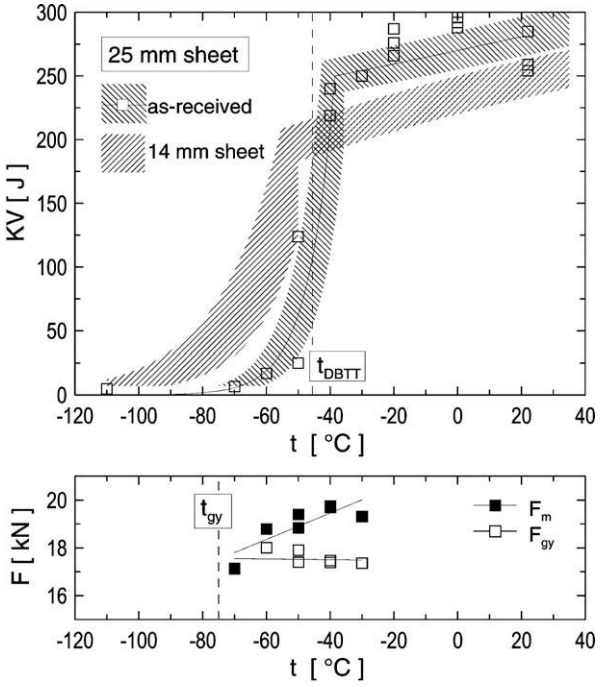

Fig. 5. Charpy impact energy temperature diagram of 25 mm sheet of Eurofer'97 in as-received state (upper – temperature dependance of impact energy, lower – thermal dependance of F_{gy} and F_m).

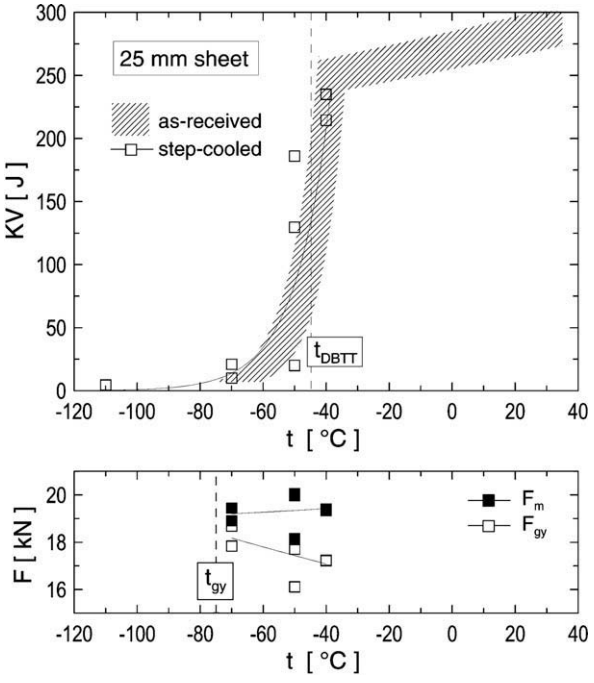

Fig. 6. Charpy impact energy temperature diagram of 25 mm sheet of Eurofer'97 in as-received state (upper – temperature dependance of impact energy, lower – temperature dependance of F_{gy} and F_m).

ations of specimens fractured near t_{gy} temperature revealed cleavage mechanism of brittle fracture initiation and propagation (see Fig. 4(b)). No reasons for observed differences in temperature dependence of impact energy were observed in the microstructure and chemical composition, despite of using two different heats of Eurofer'97 steel. The differences in chemical composition of both heats used were of the order of hundredths of wt% what is in the value as limit of analytical method used (see Table 1). The reason for Charpy impact energy variation could be find in different deformation history of two sheets of different thickness used.

No difference between temperature dependance of impact energy of 25 mm sheet in the as-received state and in state after step cooling was observed (see Fig. 6). Step cooled 25 mm sheet showed no evidences of thermal embrittlement. Impact energy of the step-cooled 25 mm sheet lied in the scatter band of the as-received 25 mm sheet. Values of t_{DBTT} temperature and t_{gy} were similar as in the case of 25 mm sheet in the as-received state and were −45 °C and −75 °C respectively. Fractographic examinations revealed no presence of intergranular fracture as a consequence of grain boundary weakening by phosphorus segregation in the case of step-cooled steel. Thermally aged material fractured near t_{gy} temperature by cleavage mechanism and fracture triggering by secondary phase was observed (see Fig. 4(c)).

Long-term thermal ageing at 500 °C/10 000 h and 600 °C/10 000 h and subsequent embrittlement of the Eurofer'97 steel described in the literature [10] led to t_{DBTT} shift by ca. +20 °C and +25 °C, respectively. The observed embrittlement was in the literature associated with the microstructural changes, especially to the partial recrystallization of martensite microstructure to the equiaxed ferrite grains. Low effort was given however to the carbide coarsening observed by Fernandez et al. [12] during 500 °C/5000 h and 600 °C/1000 h ageing and its possible influence on fracture behaviour of the Eurofer'97 steel. The growth of carbides of $M_{23}C_6$ type from 40–260 nm to 40–300 nm was observed after thermal ageing at 500 °C/5000 h and 600 °C/1000 h, respectively. In the work of Fernandez et al. [10] the segregation of phosphorus on to grain boundaries was noted after ageing at 500 °C/5000 h a 500 °C/10 000 h, it means at the lower limit of the considered exploitation range for the steel. With respect to the low phosphorus content (up to 0.005 wt%) a risk of grain boundary weakening by phosphorus segregation is very low.

4. Conclusions

The influence of thermal ageing on fracture properties of 14 mm and 25 mm sheets of Eurofer'97 steel was investigated. The thermal ageing of the Eurofer'97 steel was simulated by step cooling treatment. Charpy impact tests were performed before and after thermal ageing and impact energy, transition temperature t_{DBTT} and t_{gy} were evaluated. Impact fracture behaviour of 14 mm sheet corresponded to the literature data. t_{gy} and t_{DBTT} transition temperature of 14 mm sheet was −75 °C and −60 °C, respectively. A completely different impact fracture behaviour of 25 mm sheet in comparison with 14 mm one was observed. t_{DBTT} shift about +20 °C to the value ca. −45 °C was observed. t_{gy} transition temperature achieved value about −75 °C. No difference between temperature dependence of impact energy of 25 mm sheet in as-received state and in state after step cooling was observed. It was found, that the in as-received and step-cooled Eurofer'97 steel under the conditions of brittle fracture (near t_{gy} general yield temperature) crack initiated and propagated by cleavage mechanism with no evidences for grain boundaries weakening due to phosphorus segregation.

Acknowledgements

This work was carried out under support of Czech Science Foundation Project No. 106/08/1397, Grant Agency of the Academy of Sciences of the Czech Republic project IAA200410502 and of EURATOM Project No. IPP CR UT7 DEGR IPM2.

References

[1] R.L. Klueh, Int. Mater. Rev. 50 (2005) 287.
[2] M. Garcia-Mazario, A.M. Lancha, M. Hernandez-Mayoral, J. Nucl. Mater. 360 (2007) 293.
[3] N. Baluc, Plasma Phys. Control. Fus. 48 (2006) B165.
[4] B. van der Schaaf, F. Tavassoli, C. Fazio, et al., Fusion Eng. Des. 69 (2003) 197.
[5] A.-A.F. Tavassoli, A. Alamo, L. Bedel, et al., J. Nucl. Mater. 329–333 (2004) 257.
[6] A.-A.F. Tavassoli, J.W. Rensman, M. Schirra, K. Shiba, Fusion Eng. Des. 61&62 (2002) 617.
[7] H. Ono, R. Kasada, A. Kimura, J. Nucl. Mater. 329–333 (2004) 1117.
[8] Q. Huang, J. Li, Y. Chen, J. Nucl. Mater. 329–333 (2004) 268.
[9] J. Lapena, M. Garcia-Mazario, P. Fernandez, A.M. Lancha, J. Nucl. Mater. 283–287 (2000) 662.
[10] P. Fernandez, M. Garcia-Mazario, A.M. Lancha, J. Lapena, J. Nucl. Mater. 329–333 (2004) 273.
[11] P. Fernandez, A.M. Lancha, J. Lapena, M. Hernandez-Mayoral, Fusion Eng. Des. 58&59 (2001) 787.
[12] P. Fernandez, A.M. Lancha, J. Lapena, M. Serrano, M. Hernandez-Mayoral, J. Nucl. Mater. 307–311 (2002) 495.
[13] R. Chaouadi, J. Nucl. Mater. 360 (2007) 75.
[14] M. Rieth et al., FZKA 6911 Scientific Report, 2003.
[15] Böhler-Uddeholm heat 993393 production data.
[16] H. Hadraba, O. Nemec, I. Dlouhy, Eng. Fract. Mech. 75 (2008) 3677.
[17] J. Rensman, H.E. Hofmans, E.W. Schuring, et al., J. Nucl. Mater. 307–311 (2002) 250.
[18] J. Rensman, E. Lucon, J. Boskeljon, et al., J. Nucl. Mater. 329–333 (2004) 1113.
[19] I. Dlouhy, Z. Chlup, V. Kozak, Eng. Fract. Mech. 71 (2004) 873.
[20] M. Nevalainen, R.H. Dodds, Int. J. Fract. 75 (1995) 131.